DOI: 10.24850/j-tyca-14-04-04

Articles

Parametric models of rainfall temporal distribution at the Yabú meteorological station in Villa Clara province, Cuba

Modelos paramétricos de distribución temporal de precipitaciones en la estación meteorológica Yabú de la provincia Villa Clara, Cuba

Carlos Castillo-García[1], ORCID: https://orcid.org/0000-0002-6430-2775

Ismabel Domínguez-Hurtado[2], ORCID: https://orcid.org/0000-0002-7841-8031

Yoel Martínez-González[3], ORCID: https://www.orcid.org/0000-0002-8023-7897

[1]Universidad Central Marta Abreu de Las Villas, Santa Clara, Cuba, ccgarcia@uclv.cu

[2]Centro Meteorológico Provincial de Villa Clara, Santa Clara, Cuba, ismabel.dominguez@vcl.insmet.cu

[3]Instituto Superior de Tecnologías y Ciencias Aplicadas, La Habana, Cuba, ymg@instec.cu

Corresponding author: Carlos Castillo-García, ccgarcía@uclv.cu

Abstract

Obtaining patterns of rainfall temporal distribution through synthetic mass curves or hyetographs is a resource applied internationally to develop the design storm. In this paper, an analysis of 243 convective rainfall events of more than 25 mm that occurred in the Yabú meteorological station of Villa Clara province, Cuba in the period from 1989 to 2019, was carried out with the objective of elaborating the synthetic hyetographs characteristic of the station using Huff's method. The rainfall was classified and three types SC-T1, SC-T2, SC-T3 were identified according to the relationship between the duration of storm and the time where the highest intensities occur. The mass curves obtained for each probability of occurrence were expressed in dimensionless hyetographs, which were adjusted to the parametric models of Sherman, Wenzel and one model elaborated by the authors, which describe the distribution of the intensities with respect to time. This result allowed obtaining the intensity-frequency-duration curves for each type of storm, and each probability of occurrence. High Pearson correlation coefficients

were achieved and the model developed by the authors showed the best performance. The results indicate that the dimensionless hyetographs obtained satisfactorily reflect the phenomenon of convective rainfall in the study location.

Keywords: synthetic hyetograph, convective rainfall, pluviogram, mass curve, precipitation.

Resumen

La obtención de patrones de distribución temporal de la lluvia mediante curvas de masa sintéticas o hietogramas es un recurso aplicado a nivel internacional para elaborar la tormenta de diseño. En el presente artículo se realizó un análisis de 243 eventos lluviosos convectivos de más de 25 mm ocurridos en la estación meteorológica Yabú de la provincia Villa Clara, Cuba, en el periodo comprendido desde 1989 hasta 2019, con el objetivo de elaborar los hietogramas sintéticos característicos de la estación mediante el método de Huff. Se categorizaron las lluvias y se identificaron tres tipos SC-T1, SC-T2, SC-T3 de acuerdo con la relación entre el tiempo de duración del aguacero y el tiempo donde ocurren las mayores intensidades. Las curvas de masa obtenidas para cada probabilidad de ocurrencia se expresaron en hietogramas adimensionales, los cuales fueron ajustados a los modelos paramétricos de Sherman, Wenzel y uno propio elaborado por los autores, que describen la

distribución de las intensidades con respecto al tiempo. Este resultado permitió obtener las curvas de intensidad-frecuencia-duración para cada tipo de aguacero, y cada probabilidad de ocurrencia. Se lograron elevados coeficientes de correlación de Pearson y el modelo elaborado por los autores mostró el mejor desempeño. Los resultados indican que los hietogramas adimensionales obtenidos reflejan satisfactoriamente el fenómeno de lluvias convectivas en la localidad de estudio.

Palabras clave: curva de masa, coeficiente de retardo, hietograma sintético, pluviograma, precipitación convectiva.

Received: 07/09/2021

Accepted: 27/12/2021

Introduction

The design storm is one of the most relevant components in rainfall-runoff models because it is the starting point of any analysis at the event scale that is intended to be carried out. Chow, Maidment and Mays (1994) define a design storm in a practical way as a precipitation pattern defined to be used in the design of a hydrological system and can even be used for erosivity studies on land with potential capacity for landslides (Singh & Singh, 2020).

Rain is usually described by several parameters associated with its own characteristics (Pochwat, Słyś, & Kordana, 2017): intensity (mm/min or mm/h), precipitation sheet (mm) and its duration (min, h), However, these are not enough for their complete description, since the shape or distribution factor is essential to obtain, since it can be defining in a runoff model. Mazurkiewicz and Skotnicki (2018b) determine that there may be an increase in the peak of the discharge with an increase in the value of the advance coefficient of the storm r (or delay of the peak), which is nothing more than the relationship between the time from the start of the storm to where the greatest intensity (or greatest intensities) occurs and the total time of the storm.

In agreement with El-Sayed (2018), Dauji (2019), and Balbastre-Soldevila, García-Bartual and Andrés-Doménech (2019), there are traditionally two ways to find pattern hyetograms for design storms. The first is based on studies of the actual precipitation patterns of rainy events that occurred at a given measurement station. The Soil Conservation

Service (SCS) of the United States of the Department of Agriculture in 1986 published synthetic storms for use in that country, with durations that vary from 6 to 24 hours (Serna & Taipe, 2019), the results for 24 h are known internationally as Type I, IA, II and III (Bezak, Šraj, Rusjan, & Mikoš, 2018), which correspond to specific regions of the United States. It is recommended according to MacCuen (1989) —cited in García-Bartual and Andrés-Doménech (2017)— for basins smaller than 250 km^2, and they are applicable for any return period.

The Huff method also obtains precipitation patterns (Huff, 1990), and in recent years it has gained traction in many countries around the world. Like the models of the SCS, the Huff curves are dimensionless cumulative curves with a specific probability of occurrence (Pan, Wang, Liu, Huang, & Wang, 2017), and are widely used in rainfall-runoff models such as storm design. In practice, historical storm data is divided into four quartiles according to the normalized peak time, and each of them presents curves according to the probability of occurrence.

Several studies have adopted the Huff methodology to obtain mass curves, as well as representative synthetic hyetograms of a given locality. El-Sayed (2018) constructed the standard hyetographs for the Sinai area in the Middle East and concluded that its results are 17 % higher than those of the SCS with respect to the discharge peak in a theoretical-conceptual runoff model. Serna and Taipe (2019) carried out a very interesting study on the variation of the types of storms obtained with the

Huff method with respect to the latitude where they occurred in the Central Andes in Peru. Sumarauw, Pandey, & Legrans (2019); Duka, Lasco, Veyra Jr. and Aralar (2017); Jun, Qin and Lu (2019, as well as Priambodo, Suhardjono, Montarcihc y Suhartanto (2019) obtained patterns in several countries in Southeast Asia. Other studies in countries such as Slovenia and Poland reported by Bezak *et al*. (2018) and Mazurkiewicz and Skotnicki (2018a) carry out similar analyzes on the influence of the types of rainfall obtained in runoff models.

The second way to obtain behavioral patterns of temporal distribution of rainfall is to obtain hyetograms using Intensity-Duration-Frequency (IDF) curves. This method was initially proposed by Keifer and Chu (1957), and from this derivations have emerged that according to Watt and Marsalek —cited by Krvavica and Rubinić (2020)— can be considered in two branches: a) methods of simple geometric figures and b) methods based on frequency. Among the most used are the rectangular hyetogram, triangular hyetogram, Sifalda method, Chicago design storm and its improved variant of alternating blocks as reported by Pochwat *et al*. (2017); Balbastre-Soldevila *et al*. (2019), and García-Bartual and Andrés-Doménech (2017). The instantaneous intensity model developed by Keifer and Chu (1957), was applied by Na and Yoo (2018), to evaluate the temporal distribution of rainfall with annual maximum events in Seoul, Korea. Recently Martínez, Planos and Perdigón (2020) have obtained temporal distribution patterns in the form of hyetograms considering the origin and danger of precipitation.

The local storm phenomenon has been the cause of many flash flooding problems in small basins, such is the case of the Bélico and Cubanicay river basins in the city of Santa Clara, With the adoption of rainfall models, the aim is to predict the impacts of each type of storm on the fluvial network, the temporal variation together with the spatial one (the last one reduced almost to zero for small enough basins) allows to know exactly the location of the storms peaks of the resulting hydrograph in a given drainage system, for the adoption of opportune non-structural measures that allow safeguarding goods and resources, which are continuously damaged due to the impossibility of predicting these events.

The main objective of this contribution is to obtain the precipitation hyetograms corresponding to the Yabú meteorological station near the city of Santa Clara through the study of 31 years of records between 1989 and 2019 of rainy events greater than 25 mm in 24 h. The study is based on a unit graph of sheet versus time, which allows greater flexibility for different uses, both engineering and hydrometeorological. In this sense, three models will be evaluated from the instantaneous intensity method, from the estimation of parameters through a least square adjustment. Subsequently, the respective IDF curves will be obtained, characteristics of the station under study, to be used in a future regionalization study in future contributions.

Tecnología y Ciencias del Agua

OPEN ACCESS

Check for updates

Materials and methods

The Yabú meteorological station (Code 78343) is located in Villa Clara province, Cuba, situated at 22º 26' N and 79º 59' W, at 116.44 m above mean sea level, with the presence of a flat relief (see Figure 1), approximately 7 km from the center of Santa Clara city. It is framed on the east bank of the Sagua La Grande river basin, the largest river system in the province and where two of the most economically important reservoirs in the region are located, Embalse Palmarito and Alacranes, although it is not the only station of the basin, its privileged position in it, allows to have an accurate behavior of the climatic variables that affect the place. It began operating on September 3, 1976, the date of its first measurement record of all its own variables. It has several instruments suitable for meteorological activity, among which is the pluviometer and pluviograph:

1. Pluviometer Rain Gauge model (USWB), with measurement start date in 1976, measurements are made in millimeters (mm).

2. Pluviograph: Brand (Standard), Model (P-2), Series (281) manufactured in the former Union of Soviet Socialist Republics. (USSR), with start date of measurements in 1976.

Figure 1. Geographic location of the Yabú meteorological station, Villa Clara province, Cuba.

An analysis of 31 years of pluviographic records is carried out from 1989 to 2019 with records only interrupted in periods that do not exceed three months, due to breakage, maintenance, malfunction or poor quality of the pluviogram for reading.

n the case of the year 1990, its records were lost, which is why it is considered to start the analysis in 1989. The period from 1976 to 1988 was not included due to the intermittent absence of data due to the causes explained above, in addition to Consider further analysis of the remaining

stations in the province where the youngest of the stations begins its measurements in the late 1980s.

The pluviograms were discretized as follows:

1. Pluviogram Analyzed (PAN): Chart with the presence of more than two siphon marks, which means that in well-calibrated charts the record exceeds 20 mm and in its vast majority 25 mm. These pluviograms are digitized using mass curves.
2. Pluviogram Not Analyzed (PNA): Chart with the presence of one to two siphon marks, which ensures 10 to 20 mm of measurement in 24 hours of registration. Mass curves are not performed on these pluviograms, only the values of the sheet measured by the equipment, time measured by the equipment, average intensity of precipitation measured by the equipment and total sheet of 24 hours are obtained (the latter is a that the equipment operator writes on the chart's technical sheet, value obtained from the measurement of the pluviometer that is located less than two meters from the pluviograph, the PANs will also collect this value).
3. Lost Pluviogram (PPE): Rain data is not counted in a given period, or the equipment is defective, in some cases the 24-hour measurement is obtained, in others the exact cause of the bad measurement or another description.

Table 1 shows a summary of the obtaining of these initial data by five-year period. It should be noted that the total number of PAN does not

coincide with that of registered rainy events because on some occasions the events do not exceed 25 mm of rain and although their mass curve is digitized, they are not included in the analysis. In other cases, rain is not statistically significant for the case of this study, but it is significant for obtaining its short-term parametric IDF relationships in subsequent contributions.

Table 1. Summary of data from the pluviograms. Source: Own elaboration.

Measurement period	PAN	PNA	PPE	Days without rainfall
1989-1994	62	80	6	413
1995-1999	58	72	24	0
2000-2004	55	72	12	120
2005-2009	48	73	16	28
2010-2014	55	81	15	61
2015-2019	43	91	4	122

The analysis of the PAN and PNA discretizes the rainy events from the period 1989 to 2019 that occurred at the Yabú meteorological station

in various types of rains, which will be classified according to the use given to them in this investigation in:

1. Not significant: Frontal rainfall of 0 to 10 mm, generally present in the dry months and of which pluviograms will not be analyzed.
2. Little significant: Rain of between 10 and 25 mm, generally present in PNA, although only parameters such as average intensity, depth and time are obtained from it. A total of 409 events are quantified.
3. Significant: Rain greater than 25 mm, used to obtain Mass Curves, all the necessary data are extracted and detailed processing is carried out. They are all in PAN and a total of 243 events with durations ranging from 20 min to 285 min and sheets between 20 and 125 mm are quantified.
4. Cyclonic events: In total, the occurrence of 20 extreme cyclonic events from Lily in 1996 to Alberto in 2018 are compiled in the period, most with problems in the registry or that the level of precipitation at the station was little or not significant.

In order to obtain the temporal distribution patterns of the representative precipitations of the Yabú meteorological station, firstly, the procedures of Huff (1990) are studied, being valid to emphasize that in this case the author himself cites that, in his study elaborated in 1967, the The relationship of these unit curves could be obtained from a point station or from a record of an area from 130 to 1035 km2. He also points out that the distribution of rainfall is grouped according to the position of the moment where the maximum intensities of the event occur, which in

his opinion could occur in the first, second, third and fourth quartiles of the storm.

The review of the literature indicates that there are examples of reducing the number of quartiles, such is the case of Serna and Taipe (2019), who propose three, whose philosophy will be adopted in this study. Dauji (2019) proposes a new methodology also inspired by the Huff method that details the elaboration of synthetic hyetograms using the generalized mass curve of 95 % confidence level for each year and its result is the obtaining of a unit mass curve global, which is dimensioned with the IFD curve parameters of the study region. To elaborate the unit mass curves in this study, the following sequence of steps is proposed:

1. Obtain the dimensional mass curves of each rainy event that occurred greater than 25 mm from the study station.
2. Prepare the unit mass curve of all the events recorded in step 1, not considering in this curve the initial and final sections where the intensity is less than 0.033 mm/min considered weak (AEMET, 2015).
3. Classify the unit mass curves into three groups (Type 1, 2 and 3 respectively), according to the probabilities of occurrence (obtained for each unit value of time with intervals of 5 % using the percentile values in P10, P20, P30, … P90) and the relationship between the duration of the downpour and the time where the greatest intensities occur (coefficient of advance of the storm r). Type 1 ($r < 0.5$, early type showers), Type 2

(r ~ 0.5, centered type showers) and Type 3 (r > 0.5, delayed type showers).

4. Find the dimensionless hyetograms of Type 1, 2 and 3 respectively from the unit mass curves of step 3.
5. Obtain the adjustment parameters of parametric models of temporal distribution of rainfall in the reference station.
6. Obtain the respective curves Intensity – Duration – Frequency (IDF)

The behavioral patterns of precipitation can be represented by IDF curves (Planos, Limia, & Vega, 2005; Martínez *et al*., 2020). These curves, among multiple applications, make it easier for engineering designs of civil works, and in particular hydraulic ones, to be more reliable (Gutiérrez, Pérez, Angulo, Chiriboga, & Valdés, 2017; Balbastre, 2018), and constitute a tool for analysis and planning in the short term, medium and long terms, which has a significant weight in investment decisions and their protection. Table 2 shows a group of equations, used in hydrological practice, to estimate the intensity of precipitation. According to these equations, the intensity of precipitation decreases with the duration of the rainy event, which can be associated with a certain probability of occurrence.

Table 2. Empirical equations for IDF curves. Source: Martínez *et al*. (2020).

Author	Formulation
Talbot	$I = \frac{a}{t+b}$ (1a)
Bernard	$I = \frac{a}{t^n}$ (1b)
Sherman	$I = \frac{a}{(t+b)^n}$ (1c)
Wenzel	$I = \frac{a}{t^n+b}$ (1d)

a, *b* and *n* = data-related tuning parameters vary with the probability of occurrence.

When performing an inspection on equations (1a)-(1d), it is possible to extend their structure, considering that each adjustment parameter varies with the probability of occurrence, using the following model:

$$I = \frac{a}{(t^n+b)^c} \quad (2)$$

The use of dimensionless curves is a technical resource of excellence to make records comparable in physical-geographically homogeneous localities; to give greater certainty to other techniques such as the transposition of values and to deal with anomalous values (Martínez *et al*., 2020). To do this, firstly, the times and intensities are normalized. In this case, the duration Td and the average intensity Im for each

probability of occurrence are considered, as $I_m\,(prob) = \frac{P_{acum}(prob)}{T_d}$, when $P_{acum}(prob)$, the accumulated precipitation of a certain probability of occurrence in time T_d. In this way, the following dimensionless relationships are established $\tau = \frac{t}{T_d}$ and $i = \frac{I}{I_m}$, for time and intensity respectively and then equation (2) can be rewritten as:

$$i = \frac{a}{(\tau^n + b)^c} \tag{3}$$

In equations (1a) to (1d), (2) and/or (3), the parameters are considered constant for each probability of occurrence, regardless of the duration of rainfall. This particularity allows obtaining a linear relationship in a doubly logarithmic coordinate system that is:

$$\log \mathrm{i} = \log \mathrm{a} - \mathrm{c}\log(\tau^{\mathrm{n}} + \mathrm{b}) \tag{4}$$

However, despite the extension in complexity introduced in equations (2) and (3), it is possible that, for all durations, satisfactory results are not obtained in the regression. For this reason, an extension with a second order term is introduced in a doubly logarithmic coordinate system, that is:

$$\log i = \log a - c \log(\tau^n + b) - m \log^2 (\tau^n + b) \quad (5a)$$

or:

$$i = \frac{a}{(\tau^n + b)^{c + m \log(\tau^n + b)}} \quad (5b)$$

Note that an additional parameter m is introduced, which is particularly necessary to adjust for short duration precipitation events. Next, Table 3 shows the values that the parameters of equation (5.b) must adopt, to describe the particular cases corresponding to the IDF curve models of Talbot, Bernard, Sherman and Wenzel, previously presented in Table 3.

Table 3. Values of the parameters of equation (2) for particular cases.

Author	**Parameters**
Talbot	$n = 1$, $c = 1$, $m = 0$
Bernard	$b = 0$, $c = 1$, $m = 0$
Sherman	$n = 1$, $m = 0$ c: replaces to n in (1.c)
Wenzel	$c = 1$, $m = 0$

Source: Own elaboration from various authors.

According to the instantaneous intensity method developed by Keifer and Chu (1957), the instantaneous rain intensity R in a storm downpour can be described by the following ordinary differential equation, as a function of the intensity i of the IDF curves:

$$R = i + \tau \frac{di}{d\tau} \quad (6)$$

By applying this method to equations (1.a - 1.d) and (5.b), it can be shown that the instantaneous intensity R will be given for each parametric model as shown in Table 4.

Table 4. Dimensionless instantaneous hietograms.

Author	Formulations
Talbot	$R = \frac{a\,b}{(\zeta+b)^2}$ (7a)
Bernard	$R = \frac{a(1-n)}{\zeta^n}$ (7b)
Sherman	$R = \frac{a\,[b+(1-n)\zeta\,]}{(b+\zeta\,)^{n+1}}$ (7c)

Author	Formulations
Wenzel	$R = \frac{a\,[b+(1-n)\,\zeta^n]}{(b+\zeta^n)^2}$ (7d)
Autores	$R = \frac{a\{b+[1-c\,n-2mn\,log(b+\zeta^n)]\,\zeta^n\}}{(b+\zeta^n)^{c\,+\,m\,log(b+\zeta^n)\,+1}}$ (7e)
Autores (*m* = 0)	$R = \frac{a\,[b+(1-c\,n)\,\zeta^n]}{(b+\zeta^n)^{c+1}}$ (7f)

a, b, c, n y *m* = data-related tuning parameters, which vary with the probability of occurrence.

Source: Own elaboration from various authors.

In the previous expression, the variable ζ is introduced, which represents a time scale relative to the storm advance coefficient r, and is defined as:

$$\zeta = \begin{cases} \frac{r-\tau}{r} & 0 \leq \tau \leq r \\ \frac{\tau-r}{1-r} & r \leq \tau \leq 1 \end{cases} \qquad (8)$$

For ζ = 0 the maximum intensity R_{max} is obtained, and in this sense the parameter a can be obtained as a function of said intensity value, showing its linear proportionality in relation to said intensity value. It is valid to

emphasize that, in Bernard's model, there is a lack of definition, due to the simple structure of his equation. However, a small value can be entered on the dimensionless time scale ζ = ε, for example ε = 0.01, and this problem is approximately solved. In effect, for each particular case it will be as shown in Table 5.

Table 5. Dependence of the parameter a.

Author	Formulations
Talbot	$a = R_{max}\, b$
Bernard	$a = \frac{R_{max}\, \varepsilon^n}{(1-n)}$
Sherman	$a = R_{max}\, b^n$
Wenzel	$a = R_{max}\, b$
Autores	$a = R_{max}\, b^{c + m\, log(b)}$
Autores (m = 0)	$a = R_{max}\, b^c$

Source: Own elaboration from various authors.

In this contribution, although the analysis can be conducted for all the parametric models present in Table 4, without subtracting generality, Sherman (Ec 7.c), Wenzel (Ec. 7.d) and Ec (7.e), the latter developed by the authors. The parameters will be obtained from a non-linear fit, in such a way that the following objective function is minimized:

$$\mathrm{F.O}(\bar{p}) = \min log \sqrt{1 + \sum_{j=1}^{N} \left(R_j(\bar{p}) - R_{oj}\right)^2} \quad (9)$$

when $\bar{p}$ = vector of parameters (in a general sense $\bar{p} = [R_{max}, b, c, n, m, r]$), N = number of observations, R = simulated instantaneous intensity and R_o = instantaneous intensity recorded (observed).

Results and discussion

The application of the Huff method with the modifications proposed by Serna and Taipe (2019), leads to the following mass curves, with a 5 % increase in the time scale and dimensionless instantaneous hyetograms for each established grouping (see Figure 2).

Tecnología y Ciencias del Agua

OPEN ACCESS

Check for updates

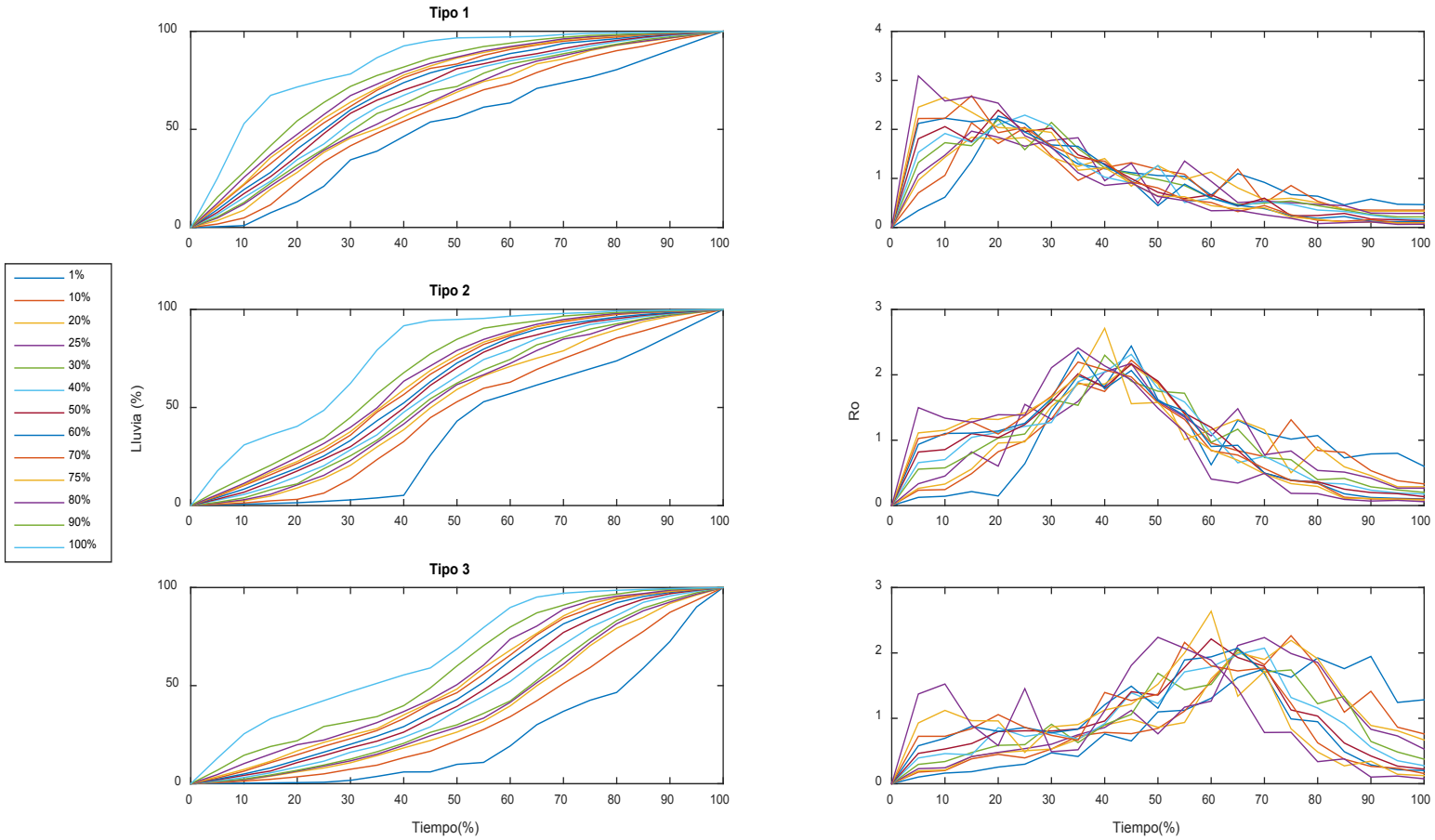

Figure 2. Pooled dimensionless instantaneous mass curves and hyetograms. Source: Own elaboration.

The parameters of the temporal distribution models of rainfall are obtained by applying the Levenberg-Marquardt method —described in detail by Gill, Murray and Wright (1981)— to minimize the objective function described by equation (9). Due to the importance it reverts to the territory, for each type of distribution and model the results are shown in Table 7, Table 8 and Table 9, characterized by satisfactory correlations based on the values of the Pearson correlation coefficient, according to the strategy followed in this contribution. It is valid to highlight, from the temporal increase of 5 %, there are a total of N = 21 pairs of data for each distribution. For a one-sided test according to degrees of freedom (N - 2), the critical value of Pearson's correlation coefficient for a 5 % level of significance is 0.369. In this sense, all the values achieved that are reported in Tables 7, 8 and 9 are statistically significant since they are higher than the critical one.

Tecnología y Ciencias del Agua

OPEN ACCESS

Check for updates

Table 7. Parameters and correlation of the Sherman model.

Prob. (%)	*R*max	*b*	*n*	*r*	Correlations Coeff. Of Pearson
Type 1 (*r* < 0.5)					
10	2.3152	0.8051	1.07	0.2016	0.5600
25	2.1842	1.1502	1.25	0.1239	0.9076
40	2.4491	0.9604	1.25	0.1660	0.8866
50	2.6833	0.8697	1.25	0.0636	0.8970
60	2.6739	0.8447	1.25	0.1641	0.8589
75	3.1079	0.6938	1.25	0.1084	0.8851
90	3.9217	0.5169	1.25	0.0527	0.9640
Type 2 (*r* ~ 0.5)					
10	2.5308	0.6468	1.01	0.4324	0.5426
25	2.4088	0.9808	1.25	0.4220	0.9260
40	2.4182	0.9683	1.25	0.3998	0.9320
50	2.5300	0.9113	1.25	0.3883	0.9510
60	2.5001	0.9350	1.25	0.3715	0.9291
75	2.5520	0.8955	1.25	0.3598	0.9055
90	2.8367	0.7676	1.25	0.3226	0.8453
Type 3 (*r* > 0.5)					
10	2.3756	0.9970	1.25	0.8927	0.5531
25	2.5551	0.8867	1.25	0.7802	0.9142
40	2.2181	1.1157	1.25	0.6848	0.8561
50	2.3718	0.9959	1.25	0.6812	0.9202
60	2.4403	0.9519	1.25	0.6275	0.9239
75	2.2467	1.0822	1.25	0.5846	0.9050
90	2.7299	0.3355	0.74	0.5260	0.7450

Source: Own elaboration.

Table 8. Parameters and correlation of the Wenzel model.

Prob. (%)	*R*max	*b*	*n*	*r*	Correlations Coeff. Of Pearson
Type 1 (r < 0.5)					
10	2.3402	0.7157	1.0003	0.2022	0.5601
25	2.2212	0.8212	0.9961	0.1232	0.9039
40	2.4918	0.6905	1.0001	0.1137	0.8951
50	2.7205	0.6169	1.0019	0.0629	0.8850
60	2.9278	0.5540	1.0056	0.0589	0.8916
75	3.4391	0.4399	1.0010	0.0560	0.9443
90	4.1019	0.3406	1.0001	0.0527	0.9531
Type 2 (*r* ~ 0.5)					
10	2.5357	0.6343	1.0004	0.4324	0.5432
25	2.4631	0.6878	1.0004	0.4228	0.9227
40	2.5259	0.6585	0.9995	0.4091	0.9316
50	2.6857	0.5966	0.9987	0.4202	0.9428
60	2.5373	0.6578	1.0005	0.4180	0.9388
75	2.6242	0.6199	1.0013	0.3619	0.8990
90	2.9401	0.5208	0.9999	0.3235	0.8365
Type 3 (*r* > 0.5)					
10	2.4723	0.6986	0.9988	0.9299	0.6725
25	2.6357	0.6103	1.0003	0.7801	0.9121
40	2.2575	0.7941	1.0001	0.6832	0.8509
50	2.4306	0.6961	0.9996	0.6812	0.9124
60	2.5085	0.6604	1.0006	0.6271	0.9157

Prob. (%)	*R*max	*b*	*n*	*r*	Correlations Coeff. Of Pearson
75	2.2916	0.7674	1.0026	0.6188	0.9285
90	2.5356	0.6244	1.0001	0.5271	0.7639

Source: Own elaboration.

Table 9. Parameters and correlation of the proposed model, Equation (7e).

Prob. (%)	*R*max	*b*	*c*	*n*	*m*	*r*	Correlations Coeff. Of Pearson
Type 1 (*r* < 0.5)							
10	2.2175	1.1874	1.1280	1.125	0.2174	0.2000	0.5687
25	2.0539	6.6532	1.2499	1.125	1.0000	0.1255	0.9133
40	2.2936	5.2155	1.2500	1.125	1.0000	0.1128	0.9226
50	2.4120	4.6426	1.2500	1.125	1.0000	0.1080	0.9362
60	2.6434	3.3379	1.0006	1.125	0.9999	0.0609	0.9376
75	2.0000	0.1178	1.0326	1.125	0.3530	0.0586	0.9893
90	2.6246	0.1000	1.0879	1.125	0.3037	0.0522	0.9911
Type 2 (*r* ~ 0.5)							
10	2.5289	0.6371	1.0000	1.125	0.0073	0.4325	0.5292
25	2.2254	5.5032	1.2500	1.125	1.0000	0.4193	0.9285
40	2.2718	5.2030	1.2500	1.125	1.0000	0.4008	0.9540
50	2.3330	4.9219	1.2496	1.125	1.0000	0.3899	0.9668
60	2.3172	5.0418	1.2500	1.125	1.0000	0.3684	0.9404
75	2.3398	4.9122	1.2500	1.125	1.0000	0.3384	0.9181
90	2.6725	0.5580	1.0000	1.125	0.2527	0.3198	0.8606
Type 3 (r > 0.5)							
10	2.2608	5.3520	1.2499	1.125	1.0000	0.9255	0.6468

Prob. (%)	*Rmax*	*b*	*c*	*n*	*m*	*r*	Correlations Coeff. Of Pearson
25	2.4432	0.7447	1.0000	1.123	0.2347	0.7809	0.9136
40	2.1011	6.2876	1.2500	1.125	1.0000	0.7234	0.9130
50	2.1813	4.8065	1.2468	1.126	0.8807	0.6813	0.9414
60	2.2753	1.8480	1.2500	1.126	0.4059	0.6288	0.9413
75	2.0824	6.3258	1.2498	1.126	1.0000	0.5895	0.9193
90	2.5356	0.6244	1.0000	1.125	0.0000	0.5271	0.7698

Source: Own elaboration.

Figure 3, Figure 4 and Figure 5 show the trends of the parametric models of temporal distribution of rainfall analyzed, as well as the corresponding IDF curves for each probability of occurrence. By simple inspection, it can be seen that there is convergence in the behavior of the results obtained. An analysis from complementary box plots of the Pearson correlation coefficient for each model with their associated probabilities is illustrated in Figure 6. From this analysis it can be deduced that the results in practical terms are similar. . However, the diagrams indicate that the model proposed by the authors, based on equation (7.e), presents the best performance in all types of hyetograms. This result is of great importance because it can be used later for a regionalization in other stations in the territory of Villa Clara province.

Tecnología y Ciencias del Agua

OPEN ACCESS

Check for updates

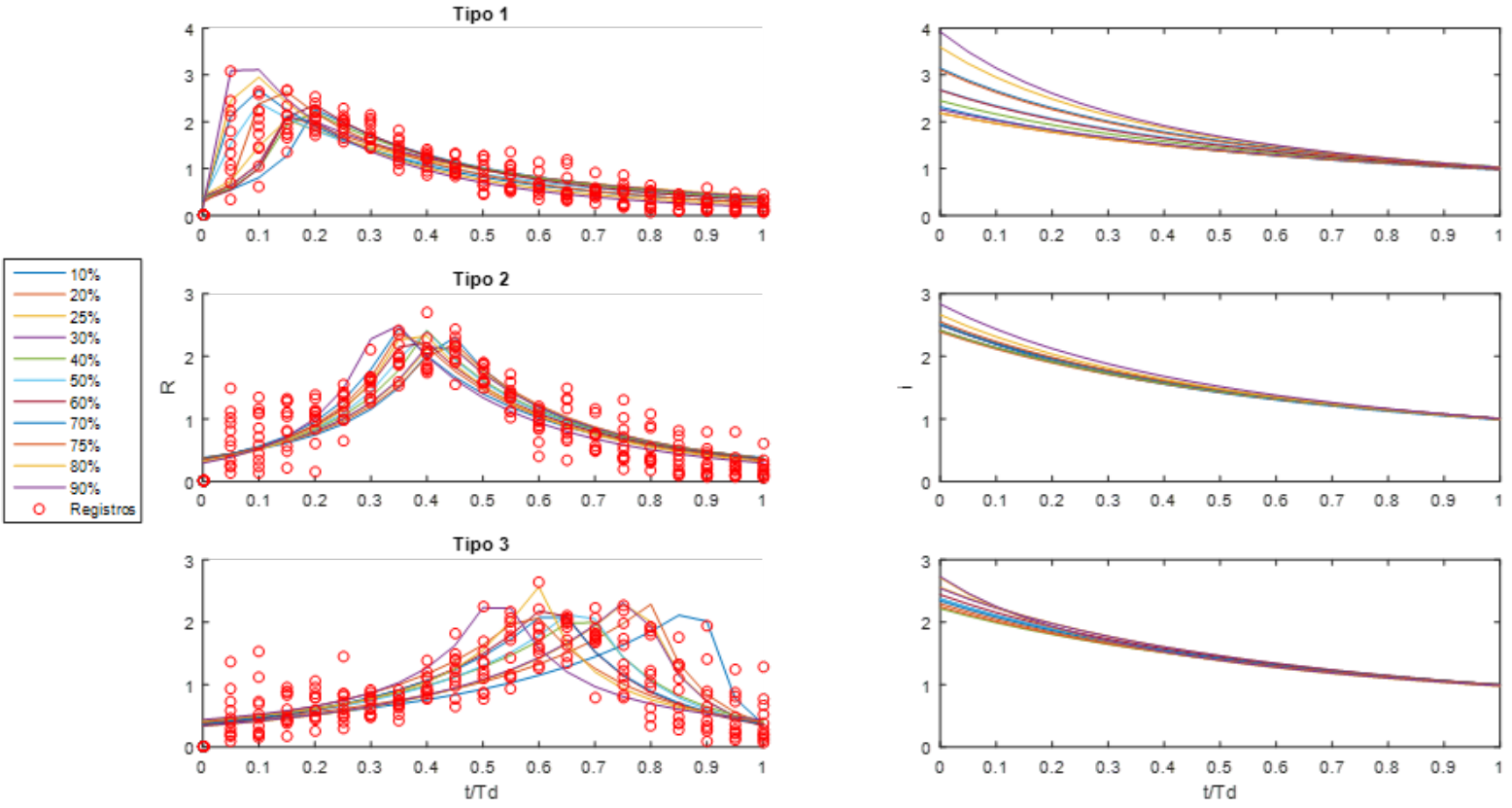

Figure 3. Fit of dimensionless instantaneous hyetograms and IDF curves grouped according to Sherman model. Source: Own elaboration.

Tecnología y Ciencias del Agua

OPEN ACCESS

Check for updates

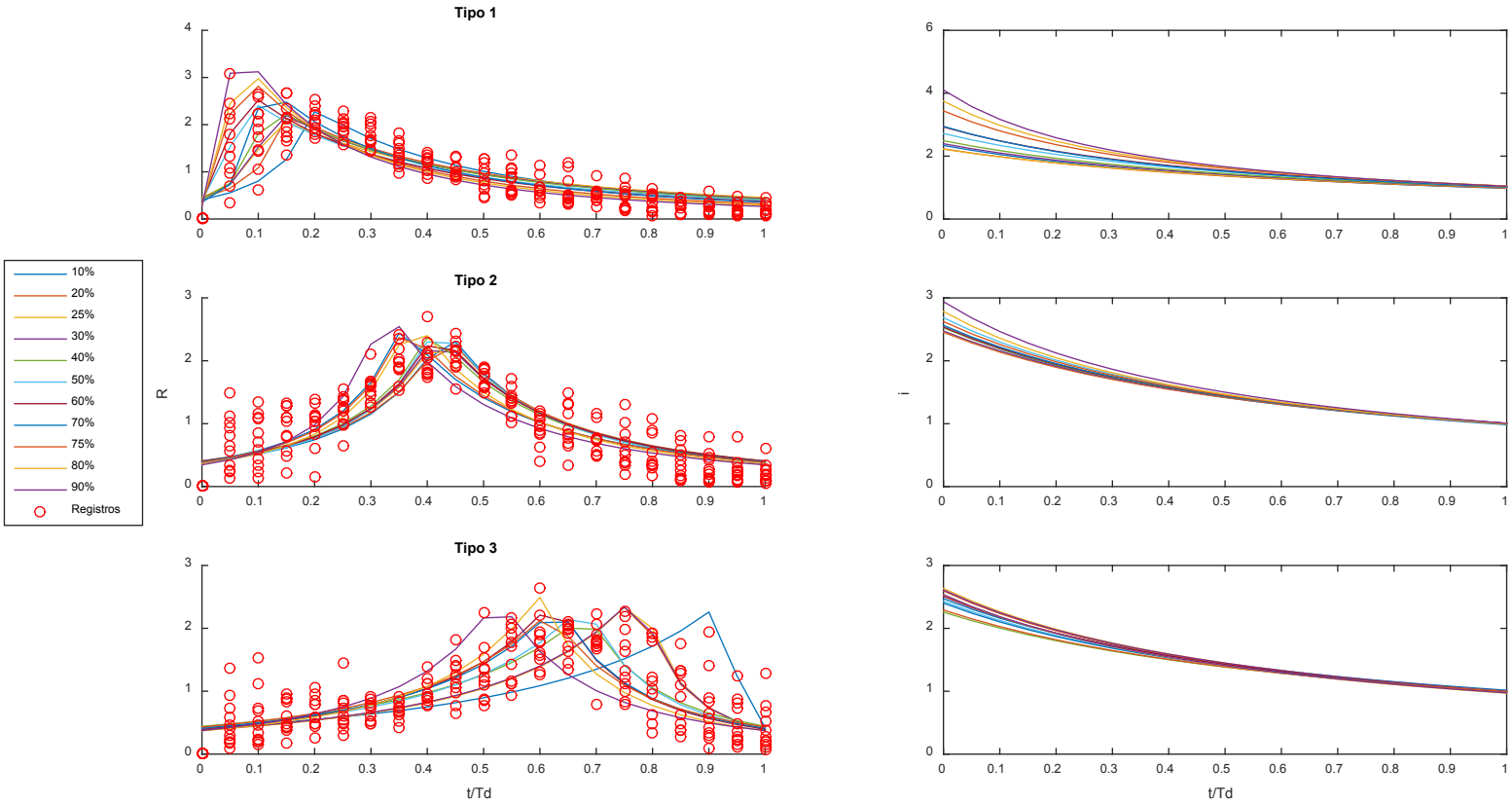

Figure 4. Fit of dimensionless instantaneous hyetograms and IDF curves grouped according to Wenzel model. Source: Own elaboration.

Tecnología y Ciencias del Agua

OPEN ACCESS

Check for updates

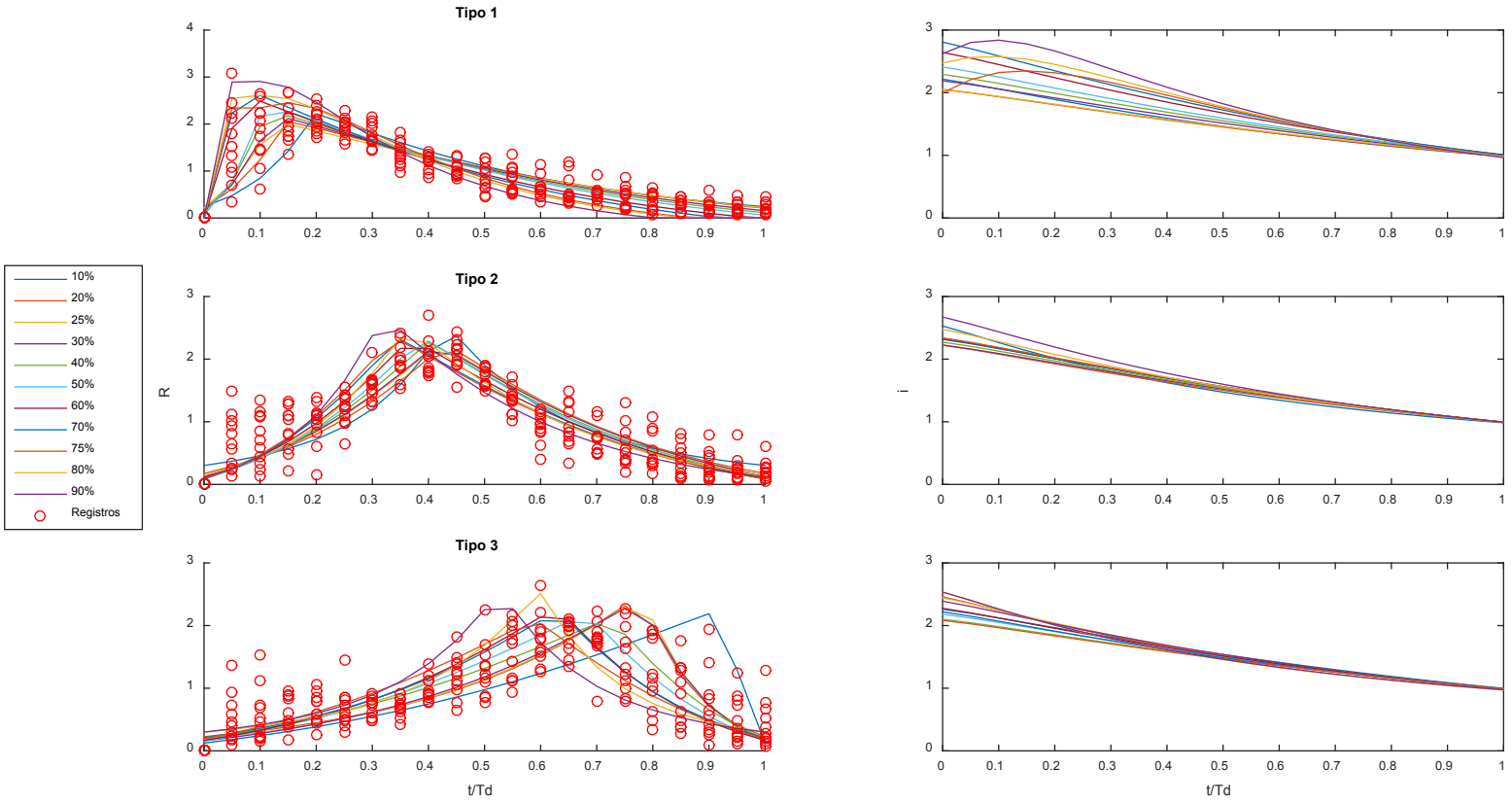

Figure 5. Adjustment of dimensionless instantaneous hyetograms and IDF curves grouped according to Equation (7e). Source: Own elaboration.

Tecnología y Ciencias del Agua

OPEN ACCESS

Check for updates

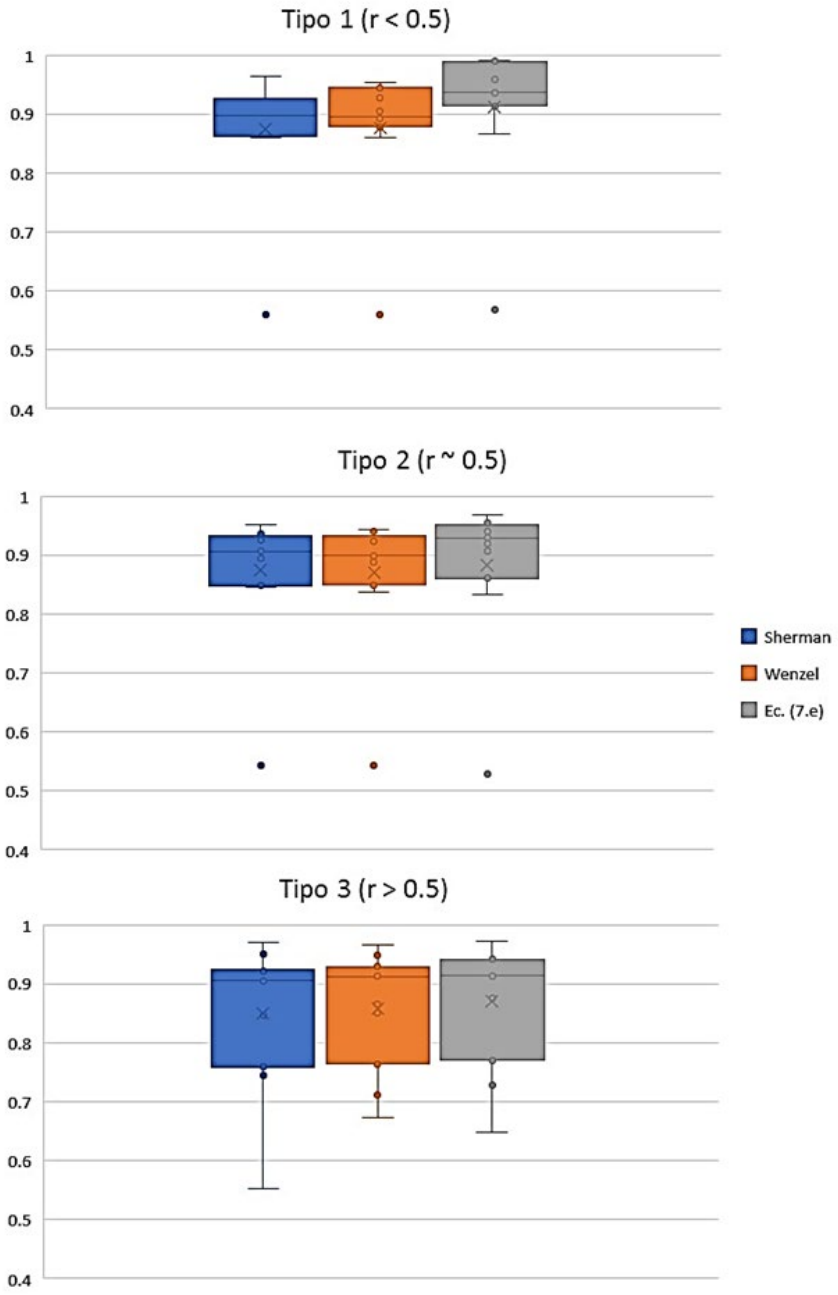

Figure 6. Box plots for the correlations of each model and type of hyetogram. Source: Own elaboration.

The IDF curves obtained by Equation (7e) present a different behavior in the vicinity of short durations, where a certain curvature is observed, mainly detected in Type 1 hietograms. As mentioned previously, the Sherman and Wenzel constitute particular cases (m = 0). Note in Table 9 that the parameter m only vanishes by fit in Type 3 hyetograms for the 90 % probabilities. All IDF curves converge at i = 1 for τ = 1. This means that $= I_m = \frac{P_{acum}}{T_d}$, which was expected when carrying out a dimensionless treatment of the pluviographic data.

The results obtained in the model presented by Equation (7e) show a high convergence for t/Td > 0.5 in the three types of storm, in addition to instantaneous maximum intensity values between 2.0 and 3.0 also for each type. , these mathematical deductions correspond to a previous analysis carried out by the authors that shows that several descriptive parameters of rainfall are similar, as shown in Table 10.

Table 10. Some comparative parameters of the rains observed in the pluviographic records in the Yabú station.

Type	Maximum intensity observed for 5 min (mm/min)	Maximum lamina observed (mm)	Average (maximum) intensity observed (mm/min)	Maximum recorded time (min)
Type I	3.33	124.6	1.33	210
Type II	2.80	118.0	1.10	285
Type III	2.50	96.8	1.40	230

Source: Own elaboration.

The analysis of the results then allows establishing the confidence limits for the proposed model according to the following points:

1. The model is valid for convective storms, in no case can the model be used in the face of cyclonic events or frontal systems, since the records exceed the time and/or sheet limit established by the analyzed data.

2. The model is valid for storms whose duration ranges between 25 and 250 continuous minutes, with intensities greater than 0.033 mm/min. In

general, all convective phenomena with more than 20 mm of precipitation meet this criterion.

3. The model is valid for sheets between 20 mm and 150 mm continuous.

4. The model is valid for average currents (L/Td) between 0.15 and 1.50 mm/min. This does not mean that intensities higher than the one established as maximum cannot be assessed, but discretion is recommended in the results.

Conclusions

The mass curves of rainy events greater than 25 mm accumulated in the Yabú station were obtained in this contribution. Data were normalized and classified into 3 types of patterns: Type 1 ($r < 0.5$, early-type downpours), Type 2 ($r \sim 0.5$, center-type downpours) and Type 3 ($r > 0.5$, delayed-type downpours), being possible to find the respective hyetograms.

Two existing models in the literature were compared and analyzed, Sherman and Wenzel. A third more general model was developed by the authors and incorporated into the process of analysis and comparison during the parametric adjustment of these to obtain empirical - analytical patterns of temporal distribution of rainfall in the reference meteorological station, the IDF curves of each model were obtained in parallel form,

It was much more flexible by having a greater number of parameters, being able to reproduce the behavior of the hyetograms of each probability with the minimum errors. These results seem to suggest that its application can be extended to other existing stations in the Villa Clara territory, which will allow regionalizing the temporal distribution model of rainfall developed here. Due to the importance it reverts to engineering and hydrological practice, it will be addressed in future research.

Acknowledgments

The authors are deeply grateful to Villa Clara Provincial Meteorological Center, for the support in the development of the investigations, which has been commendable and worthy, despite the harsh conditions imposed by the Covid-19 pandemic that affects the country. Our thanks also to Ing. Diego Emilio Abreu Franco for his constant support and advice on issues related to research and also our thanks to the Hydraulic Engineering students of the Marta Abreu Central University of Las Villas:

José Solis Quintana, Alejandro Marrero, Jose Manuel Alba Bacallao and Roberto Fernández.

References

AEMET, Agencia Estatal de Meteorología de España. (2015). *Manual de uso de términos meteorológicos*. Madrid, España: Agencia Estatal de Meteorología de España. Recovered from http://www.aemet.es/es/eltiempo/prediccion/ provincias/ayuda

Balbastre, R. (2018). *Análisis comparativo de metodologías de cálculo de tormentas de diseño para su aplicación en hidrología urbana* (tesis de maestría). Universidad Politécnica de Valencia, España. Recovered from https://riunet.upv.es/handle

Balbastre-Soldevila, R., García-Bartual, R., & Andrés-Doménech, I. (2019). A comparison of design storms for urban drainage system applications. *Water*, 11(4), 1-15. DOI: 10.3390/w11040757

Bezak, N., Šraj, M., Rusjan, S., & Mikoš, M. (2018). Impact of the rainfall duration and temporal rainfall distribution defined using the Huff curves on the hydraulic flood modelling results. *Geosciences*, 8(2), 1-15. DOI: 10.3390/geosciences8020069

Chow, V. T., Maidment, D., & Mays, L. (1994). *Hidrología aplicada*. Santafé de Bogotá, Colombia: McGraw-Hill Interamericana, S. A.

Dauji, S. (2019). Novel data-driven approach for development of synthetic hyetograph. *Journal of Hydrologic Engineering*, 24(10), 06019007. DOI: 10.1061/(ASCE)HE.1943-5584.0001846

Duka, M., Lasco, J. D., Veyra Jr., C., & Aralar, A. (2017). Comparative assessment of different methods in generating design storm hyetographs for the Philippines. *Journal of Environmental Science and Management*, 21(1), 82-89.

El-Sayed, E. A. H. (2018). Development of synthetic rainfall distribution curves for Sinai area. *Ain Shams Engineering Journal*, 9(4), 1949-1957. DOI: 10.1016/j.asej.2017.01.010

García-Bartual, R., & Andrés-Doménech, I. (2017). A two-parameter design storm for Mediterranean convective rainfall. *Hydrology and Earth System Sciences*, 21(5), 2377-2387. DOI: 10.5194/hess-21-2377-2017

Gill, P. E., Murray, W., & Wright, M. H. (1981). *Practical optimization*. London, UK: Academic Press.

Gutierrez, J., Pérez, F., Angulo, G., Chiriboga, G., & Valdés, L. (2017). *Determinación de las curvas de intensidad-frecuencia-duración (IDF) para la ciudad de Cartagena de Indias en Colombia durante el periodo comprendido entre los años 1970 y 2015*. 15th LACCEI International Multi-Conference for Engineering Education, and Technology: "Global Partnerships for Development and Engineering Education", 19-21 July 2017, Boca Raton, USA. Recovered from https://www.researchgate.net/publication/318574137

Huff, F. A. (1990). *Time distributions of heavy rainstorms in Illinois* (Circular No. 173). Recovered from https://www.isws.illinois.edu

Jun, C., Qin, X., & Lu, W. (2019). *Temporal pattern analysis of rainstorm events for supporting rainfall design in a tropical city*. Conferencia presentada en New Trends in Urban Drainage Modelling, Cham, Suiza. DOI: 10.1007/978-3-319-99867-1_64

Keifer, C. J., & Chu, H. H. (1957). Synthetic storm pattern for drainage design. *Journal of the Hydraulics Division*, 1957, 83, 1-25. Recovered from https://www.ascelibrary.org/doi/pdf

Krvavica, N., & Rubinić, J. (2020). Evaluation of design storms and critical rainfall durations for flood prediction in partially urbanized catchments. *Water*, 12(7), 1-20. DOI: 10.3390/w12072044

Martínez, Y., Planos, E., & Perdigón, D. (2020). Hietogramas adimensionales para ciclones tropicales que afectan al archipiélago cubano. *Ingeniería Hidráulica y Ambiental*, 41(2), mayo-agosto, 48-63.

Mazurkiewicz, K., & Skotnicki, M. (2018a). A determination of the synthetic hyetograph parameters for flow capacity assessment concerning stormwater systems. *E3S Web Conference*, 45, 00053. DOI: 10.1051/e3sconf/20184500053

Mazurkiewicz, K., & Skotnicki, M. (2018b). The influence of synthetic hyetograph parameters on simulation results of runoff from urban catchment. *E3S Web Conference*, 30, 01018. DOI: 10.1051/e3sconf/20183001018

Na, W., & Yoo, C. (2018). Evaluation of rainfall temporal distribution models with annual maximum rainfall events in Seoul, Korea. *Water*, 10, 1468. DOI: 10.3390/w10101468

Pan, C., Wang, X., Liu, L., Huang, H., & Wang, D. (2017). Improvement to the Huff curve for design storms and urban flooding simulations in Guangzhou, China. *Water*, 9(6), 1-18. DOI: 10.3390/w9060411

Planos, E., Limia, M., & Vega, R. (2005). *Intensidad de las precipitaciones en Cuba* (informe científico). La Habana, Cuba: Instituto de Meteorología.

Pochwat, K., Słyś, D., & Kordana, S. (2017). The temporal variability of a rainfall synthetic hyetograph for the dimensioning of stormwater retention tanks in small urban catchments. *Journal of Hydrology*, 549, 501-511. DOI: 10.1016/j.jhydrol.2017.04.026

Priambodo, S., Suhardjono, S., Montarcih, L., & Suhartanto, E. (2019). Hourly rainfall distribution patterns in Java island. *MATEC Web Conference*, 276, 04012. DOI: 10.1051/matecconf/201927604012

Serna, J. R. V., & Taipe, C. L. R. (2019). Determination of storm profiles in the Central Andes of Peru. *E-proceedings of the 38th IAHR World Congress*, Sept. 2019, Panamá, DOI: 10.3850/38WC092019-1859

Singh, J., & Singh, O. (2020). Assessing rainfall erosivity and erosivity density over a western Himalayan catchment, India. *Journal of Earth System Science*, 129(1), 97. DOI: 10.1007/s12040-020-1362-8

Sumarauw, J. S. F., Pandey, S. V., & Legrans, R. R. I. (2019). Hourly rainfall distribution pattern in the northern coast of Bolaang Mongondow. *Journal of Sustainable Engineering: Proceedings Series*, 1(1), 75-83. DOI: 10.35793/joseps.v1i1.10